

Experimental and Numerical Characterization of Pullout Behavior of Hooked Steel Fibers in Ultra-High Performance Cementitious Matrix

Author(s) & Affiliation: Congrui Jin¹, Mengxi Du², Jun Feng², Xinwei Zhou³, Gianluca Cusatis^{2*}

¹ Department of Mechanical Engineering, State University of New York at Binghamton, Binghamton, NY 13902; ² Department of Civil Engineering, Northwestern University, Evanston, IL 60208; ³ Engineering and Software System Solutions, Inc. (ES3), San Diego, CA 92101.

Abstract: Steel fiber is the most common type used to reinforce concrete. Although a large number of research studies have been conducted to investigate the pullout mechanism of straight steel fibers, experiments have shown that to improve the compressive concrete strength, flexural strength, and shrinkage, deformed steel fibers are more effective than straight fibers due to mechanical anchorage created by the deformed shape. While interface debonding and frictional sliding are the two main mechanisms controlling the pullout of straight fibers, additional mechanism due to fiber straightening during the pullout process must be taken into account for mechanically deformed fibers, which introduces additional complexity on the pullout response, and thus the analytical and numerical modelling of the pullout mechanism of deformed fibers has been a difficult task. There still exist no models in which the heterogeneous nature of the concrete is considered to characterize the pullout process of mechanically deformed steel fibers. As first proposed by Cusatis, fiber reinforced concrete is analyzed by a multi-scale model, called LDPM-F, in which the fine-scale fiber-matrix interaction is solved independently and the overall response is analyzed in a 3D meso-scale framework based on the recently formulated lattice discrete particle model (LDPM). LDPM is a realistic 3D model of concrete meso-structure developed by Cusatis et al., which has been extensively calibrated/validated under a wide range of quasi-static and dynamic loading conditions, showing superior capabilities in predicting qualitative and quantitative behavior of concrete. As a natural extension for this discrete model to include the effect of dispersed fibers as discrete entities within the meso-structure, LDPM-F incorporates this effect by modeling individual fibers, randomly placed within the framework according to a given fiber volume fraction. In this study, LDPM-F is herein extended to simulate fibers with hooked ends which, up to the present, represent the most widely used steel fibers' geometries used in concrete reinforcement. To calibrate and validate the proposed model, a tensile fiber pullout test has been designed and conducted on CORTUF, an ultra-high-performance concrete recently developed and characterized at the Geotechnical and Structures Laboratory (GSL), United States Army Engineer Research and Development Center (ERDC), which was designed to develop ultra-high compressive strength while maintaining workability and production economy.

Keywords: Steel fiber; Hooked fiber; Ultra-high performance concrete; Numerical simulation

Introduction

Concrete is by nature a brittle material that exhibits low toughness and poor resistance to cracking. To improve the mechanical properties of concrete, fiber reinforced concrete has been developed, which is defined as concrete containing dispersed randomly oriented short fibers. The main role of dispersed fibers is to restrain crack propagation whichever directions the cracks form, thus compared to plain concrete, endowing substantially higher energy absorption capacity and toughness. This beneficial effect can be attributed to fiber bridging through the fiber pullout process, which is the main mechanism of fiber reinforcement. Fiber reinforced composites contain fiber, matrix, and inter-phase interface, and their ability to resist tensile forces is dependent on the mechanical and chemical properties of these constituents. A part of the tensile force is resisted by the matrix, while the other part by the fibers. The additional resistance the fiber reinforcing provides is determined by the stress transfer at the interface of the fiber and the matrix. In order for the fiber to have any crack bridging ability, the dissipated energy during pull-out must be considerably higher than the fracture energy of the matrix. Before any cracking has taken place, elastic stress transfer is dominant, and then at more advanced stages of loading, debonding across the interface usually takes place with the frictional slip governing stress transfer at the interface, and thus the mechanical properties of fiber reinforced concrete are sensitively influenced by the bond characteristics at the interface. Therefore, it is of great importance to study the bond properties between the matrix and fiber prior to examining the various mechanical properties of fiber reinforced concrete, especially for an ultra-high performance cementitious matrix, where the role of fibers is critical to ensure strain hardening or softening behavior, post-peak structural ductility, and energy absorption capability, which are the quantities usually valued by civil engineers for safety reasons. Fiber composites are classified into four scales to simplify failure response investigation: 1) molecular, 2) micro, 3) meso, and 4) macro scales (Cantwell and Morton, 1991). The molecular level investigates the destruction of the chemical bond in the debonding process, the micro scale is focused on factors affecting load transfer between the fiber and matrix (bond strength, interfacial shear stress, critical energy release rate, etc.), the emphasis of the mesoscale is the fiber orientation and spacing, and the investigation of the whole composite is categorized at the macro level. This study focuses on the micro and meso scales of the failure response of the composite.

Background

Steel fiber is the most common type used to reinforce concrete. Although a large number of research studies have been conducted to investigate the pullout mechanism of straight steel fibers (Laranjeira et al., 2010; Lee et al., 2010; Leung and Shapiro, 1999; Naaman et al., 1991), experiments have shown that to improve the compressive concrete strength, flexural strength, and shrinkage, deformed steel fibers are more effective than straight fibers (Banthia and Trottier, 1994; Ezeldin and Lowe, 1991) due to mechanical anchorage created by the deformed shape, and thus it is not surprising that almost all commercially available steel fibers at present are mechanically deformed (Banthia and Trottier, 1994), such as hemi-circular, hooked, and corrugated fibers. While interface debonding and frictional sliding are the two main mechanisms controlling the pullout of straight fibers, additional mechanism due to fiber straightening during the pullout process must be taken into account for mechanically deformed fibers, which introduces additional complexity on the pullout response, and thus the analytical and numerical modelling of the pullout mechanism of deformed fibers has been a difficult task. Apart from

experimental observations, there are only a few models that attempted to account for the mechanical deformation (Laranjeira et al., 2010; Alwan et al., 1999; Sujivorakul et al., 2000; Georgiadi-Stefanidi, 2010). Frictional pulley model to predict the pullout force of hooked steel fibers was presented by Alwan et al. in 1999. Straight fiber pullout model was extended to model the effect of mechanical anchorage by adding a nonlinear spring at the end of the fiber (Sujivorakul et al., 2000). Both 3D and 2D finite element models were developed to simulate the pullout of hooked steel fibers from high-strength cementitious matrix (Georgiadi-Stefanidi, 2010). Analytical model to predict the pullout response of inclined hooked steel fibers was provided by Laranjeira et al. in 2010.

Despite the valuable understanding provided by the above-mentioned models, there still exist no models in which the heterogeneous nature of the concrete is considered to characterize the pullout process of mechanically deformed steel fibers. As first proposed by Cusatis et al. (Cusatis et al., 2010; Schauffert et al., 2012a; Schauffert et al., 2012b), fiber reinforced concrete is analyzed by a multi-scale model, called LDPM-F, in which the fine-scale fiber-matrix interaction is solved independently and the overall response is analyzed in a 3D meso-scale framework based on the recently formulated lattice discrete particle model (LDPM). LDPM is a realistic 3D model of concrete meso-structure developed by Cusatis et al. (Cusatis et al., 2011a), which has been extensively calibrated/validated under a wide range of quasi-static and dynamic loading conditions, showing superior capabilities in predicting qualitative and quantitative behavior of concrete (Cusatis et al., 2011b). As a natural extension for this discrete model to include the effect of dispersed fibers as discrete entities within the meso-structure, LDPM-F incorporates this effect by modeling individual fibers, randomly placed within the framework according to a given fiber volume fraction. LDPM-F has many salient and unique features, e.g., it is a multi-scale discrete model in which the effect of embedded fibers on the structural response is based directly on the micro-mechanics of the fiber-matrix interaction, and it has the ability to simulate not only tensile fracturing but also multi-axial compressive loading. However, the model does not include the additional frictional effects of deformed fibers on the composite. In this study, LDPM-F is herein extended to simulate fibers with hooked ends which, up to the present, represent the most widely used steel fibers' geometries used in concrete reinforcement (Laranjeira et al., 2010).

The effectiveness of a given fiber as a medium of stress transfer is often assessed by using a single fiber pullout test, where the fiber slip is monitored as a function of the applied load on the fiber (Banthia and Trottier, 1994), but some available research suggests that no correlation exists between the behavior of fiber in a single fiber pullout test and its behavior in a real composite (Hughes and Fattuhi, 1975). Therefore, in this study, to calibrate and validate the proposed model, a tensile fiber pullout test has been designed and conducted on CORTUF, an ultra-high-performance concrete recently developed and characterized at the Geotechnical and Structures Laboratory (GSL), United States Army Engineer Research and Development Center (ERDC) (Roth et al., 2009). CORTUF was designed to develop ultra-high compressive strength while maintaining workability and production economy. CORTUF can be broadly characterized as a reactive powder concrete, which are composed of fine aggregates and pozzolanic powders but do not include coarse aggregates like those found in conventional concrete. The maximum particle size in CORTUF is limited to that of the silica sand, which has a maximum size of approximately 0.6 mm.

Testing Methods

The mix proportion adopted in this study is summarized in Table 1 and is applied identically to all the tested matrices. Each batch consists of 8 CORTUF beams with nominal dimensions of 25.4 mm × 25.4 mm × 127 mm cast in aluminum molds. For each batch, we also make 10 CORTUF cubes of nominal dimensions of 25.4 mm × 25.4 mm × 25.4 mm on which compression tests and Brazilian tests are conducted on the date when the tension tests are performed (approximately at 28 days). The tested cubes have an average mass density of 2301 kg/m³, an average compressive strength of 157.5 MPa, and an average tensile strength of 9.5 MPa.

Table 1. Mix Design of CORTUF

Material	Proportion by Weight
Cement	1
Sand	0.967
Silica Flour	0.277
Silica Fume	0.389
Superplasticizer	0.0171
Water (Tap)	0.208

Three different configurations are designed for the tension tests: Type 1: notched unreinforced specimen; Type 2: notched fiber reinforced specimen; and Type 3: split fiber reinforced specimen. To investigate the effect of the interaction between fibers, Type 2 and Type 3 are made with different numbers of embedded fibers, as shown in Figure. 1. For fiber reinforced specimens, i.e., Type 2 and Type 3, fibers embedded in the matrix are hooked steel Dramix ZP305 with 0.55 mm diameter, cross sectional area of 0.2376 mm², 30 mm nominal length, and a reported Young's modulus and tensile strength of 210, 000 MPa, and 1100 MPa, respectively. Four different cases are considered for Type 2 and Type 3: 1-fiber, 2-fiber, 4-fiber, and 8-fiber cases, in which the fiber cross-sectional area fractions are 0.04%, 0.07%, 0.15%, and 0.29%, respectively. The nominal position of the fibers for each case is shown in Figure 1. The deviation between actual and nominal position is recorded at the end of each test, i.e., after the completion of the fiber pullout process, and the actual position of the fibers will be used in the numerical simulations. The results obtained from the cases where the actual position of the fiber is significantly deviated from its nominal position (more than 3 mm in either vertical or horizontal direction) are not presented in this study. Great care is taken to ensure that all the fibers' orientations are parallel to each other. For the purpose of comparison between different types of fibers, some tests have been performed on specimens with straight fibers having the same diameter and length.

For notched specimens, i.e., Type 1 and Type 2, steel plates of nominal dimensions of 25.4 mm × 6.35 mm × 0.6 mm are glued onto the middle of the aluminum mold on one side to pre-notch the specimens. Great care is taken to ensure that the notch is perpendicular to the specimen axis. For notched fiber reinforced specimens, i.e., Type 2, concrete is first poured into the mold, and then accurately spaced and aligned fibers are carefully added by using tweezers. Then the additional concrete is poured over the fiber and lightly vibrated to remove excess air bubbles. The split reinforced specimens, i.e., Type 3, are obtained by using a layer of cardboard of

nominal dimensions of 25.4 mm × 25.4 mm × 1.0 mm connected with the fibers, placed right in the middle of the mold to separate it into two halves. The fibers are threaded through the cardboard, which is attached to the molds prior to casting.

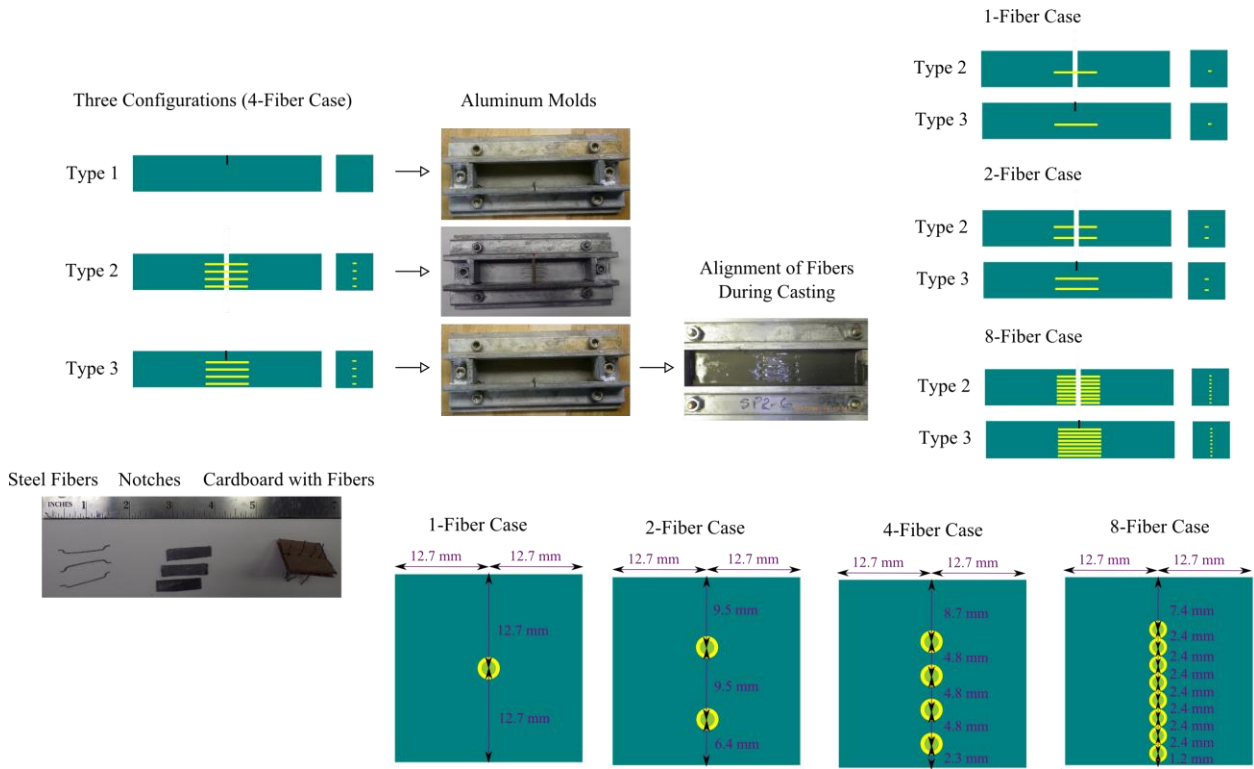


Figure 1. Three different configurations used in the experiment and the nominal positions of the fibers in each case.

After casting, the specimens are then stored in humidity room with a controlled temperature of 22 °C and 100% humidity. Specimens are demolded within 24 to 48 hours, and at 7 days of age, are submerged in a hot water bath with a nominal temperature of 90 °C for 7 days.

The preparation process of the specimens can be briefly described as follows. First, the specimens are taken out of the hot water bath and kept dry prior to testing. Each specimen’s surfaces are then carefully polished and cleaned. Steel blocks, placed into a metal frame created for this experiment, are adhered to the specimen using Loctite E-60HP Hysol Epoxy Structural Adhesive, which achieves a tensile strength of about 35 MPa and a bond strength between 4 and 8 MPa. To ensure that the crack propagates along the notch, the specimen is placed offset from the line of action of loading. The dimension of the specimen is shown in Figure 2. Second, clamps are used to ensure a successful, properly aligned final assembly. Third, the specimen is taken out of the frame after the epoxy is allowed to dry at least 72 hours, and all the dimensions of the assembly are accurately measured before testing. Since DIC technique is applied in the experiments, the middle region of the specimen of nominal dimensions of 25.4 mm × 40.00 mm is prepared with a speckle pattern. The base coat is a thin layer of white paint created by using Krylon Enamel Spray Paint, and then a speckle pattern is made by creating a black mist paint of Montana Spray Paint. To apply the black mist of paint, it is essential to keep approximate two feet of distance between specimen and spray can. The pattern is made as thin as possible. Finally, the extensometer is positioned astride the notch at mid-span.

Tension tests are carried out with a closed-loop hydraulic testing machine with a capacity of 90 kN. During each test, load, stroke, and crack mouth opening displacement (CMOD) are measured and recorded with a data acquisition system. A general view of the experimental setup is shown in Figure 3. The direct tensile test setup is designed with a so-called pin-fixed ends in order to avoid secondary flexural stress as well as to assure the centricity of loading. However, great care during operation needs to be taken to assure precise alignment.

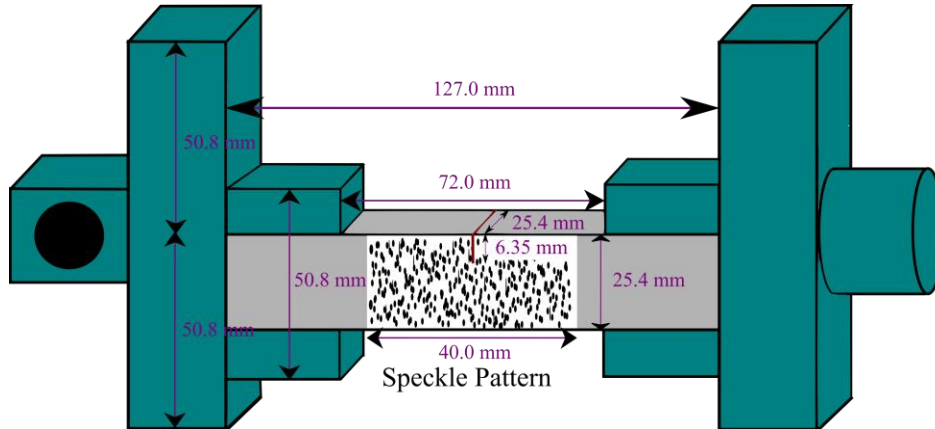


Figure 2. Dimensions of the specimen.

Computer-Controlled MTS Testing Digital Image Correlation

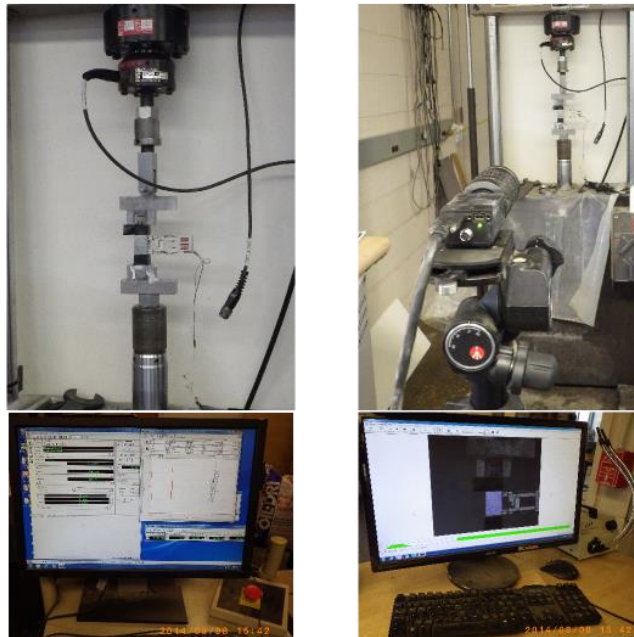


Figure 3. Experimental setup.

The tests are performed up to a complete pullout of the fibers, i.e., a 15.0 mm CMOD. The test is first under CMOD control, and the loading rate of the extensometer is 4.0×10^{-5} mm/s when CMOD is smaller than 0.02 mm, and then becomes 3.0×10^{-4} mm/s when CMOD is between 0.02 mm and 2.0 mm, and then increases to 2.0×10^{-3} mm/s when CMOD is between 2.0 mm and 3.5 mm. The test is then switched to stroke control, and the loading rate is increased to 5.0×10^{-3} mm/s until the completion of the test.

Results

In all the performed uniaxial tensile tests, the cracking occurred along the notched plane or the cardboard; hence the desired crack localization has been assured. Typical test results for three different configurations for the 4-fiber case are reported in Figure 4. At least three specimens are tested for each configuration to study the variation of experimental results.

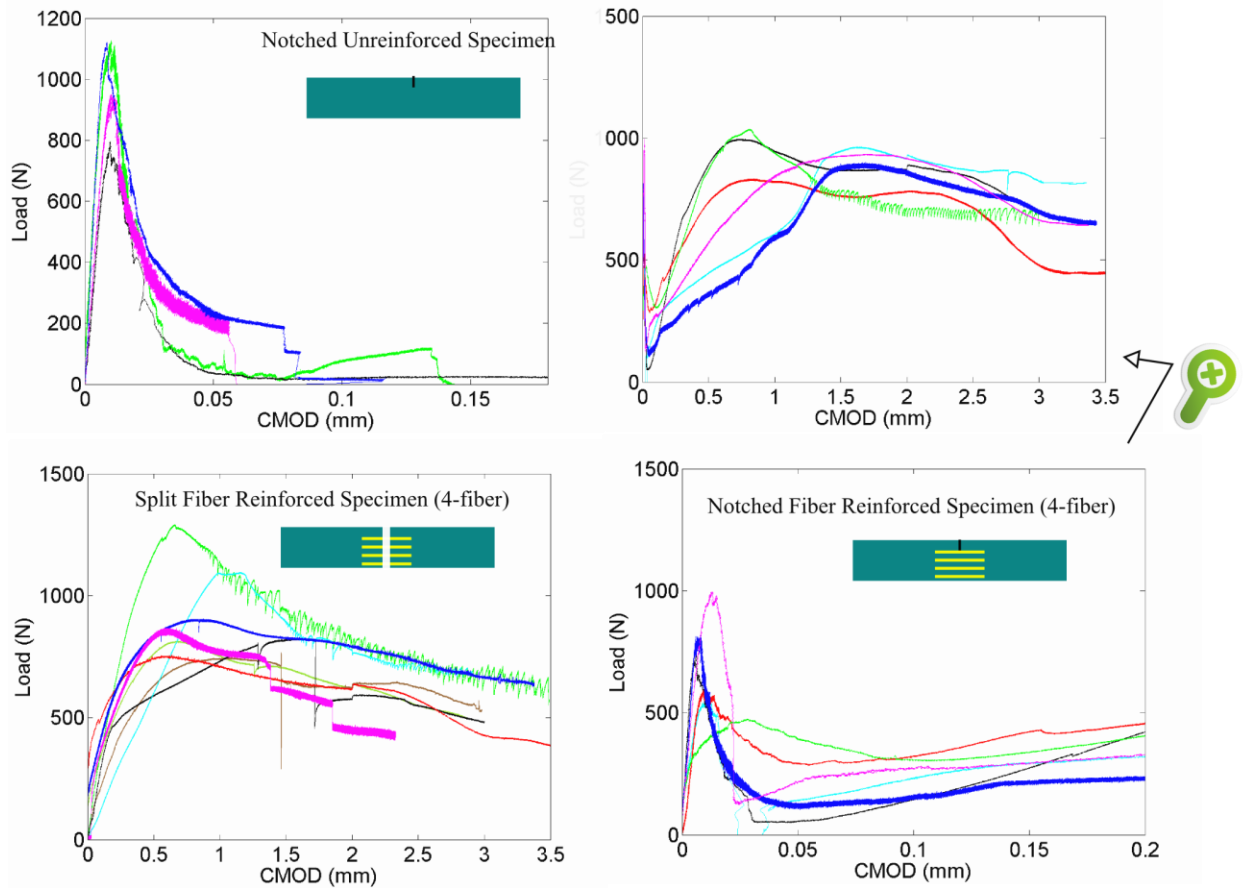


Figure 4. Test results for load vs. CMOD curves for three different configurations for the 4-fiber case.

For Type 1, the load-CMOD curve is almost linear up to the peak load at crack initiation. Only just before the peak load some nonlinearity is observed. The cracking peak load is about 930 N at which CMOD is about 0.009 mm. Once the first crack occurs in the concrete, the load suddenly decreases up to a crack width about 0.05 mm. The results demonstrate the capability of the test to obtain snap-back behavior of pre-notched specimens through steady crack propagation and controlled loading. For Type 3, the peak load appears much later with CMOD being about 1.0 mm, which is then followed by a smooth drop in the residual stress. The value of the peak load is about 267 N for the 1-fiber case, 460 N for the 2-fiber case, about 910 N for the 4-fiber case, and about 1643 N for the 8-fiber case. The results for Type 2 can be regarded as the result of a superposition of Type 1 and Type 3. It can be seen that after concrete cracking initiation, the load suddenly decreases to about 150 N up to a crack width about 0.05 mm, and beyond this crack width, notched fiber reinforced specimens and notched unreinforced specimens start to

behave in a completely distinct way: a post-peak strain hardening is observed in the fiber reinforced specimens. It indicates that in the elastic phase the contribution of fibers is rather negligible, and after crack initiation, the role of the fibers becomes more important in bridging the stresses across the crack surfaces, improving the post-cracking behavior.

Discussion and Simulation

To better understand the fiber pullout behavior, the current work formulates a high fidelity micro-mechanical model to simulate fiber inclusions in concrete. Unlike LDPM-F, the proposed model explicitly simulates each fiber as a series of beam elements which are connected head-to-tail. Such beam elements are expected to simulate the down-to-earth fiber-matrix interaction mechanisms during the fiber pullout process. Instead of using interface elements, the coupling between fiber elements and matrix elements is imposed by kinematic constraints; the interfacial bond-slip relation is modeled by phenomenological constitutive equations. The new fiber-matrix interaction model is characterized by simulating the entire fiber pullout process, and is validated against experiment results obtained from fiber pullout tests performed on CORTUF.

To simulate the fiber sliding inside the concrete matrix, a so-called slideline constraint between the fiber and the matrix is introduced, and implemented based on the updated Lagrangian algorithm. As shown in Figure 5, the concrete is simulated by discrete elements of LDPM, an edge list (the slideline) represents the geometry of the tunnel where the fiber sits in, and the fiber is explicitly modeled by Euler beam elements. The edge list, which is used to guide the pullout process, is spatially tied to the LDPM elements by master-slave constraints, with the concrete mesh being the master and the edge list being the slave. At the beginning of a simulation, the tunnel edge list and the fiber beam list perfectly overlap. The edge list deforms consistently with the concrete specimen as the fiber is being pulled out.

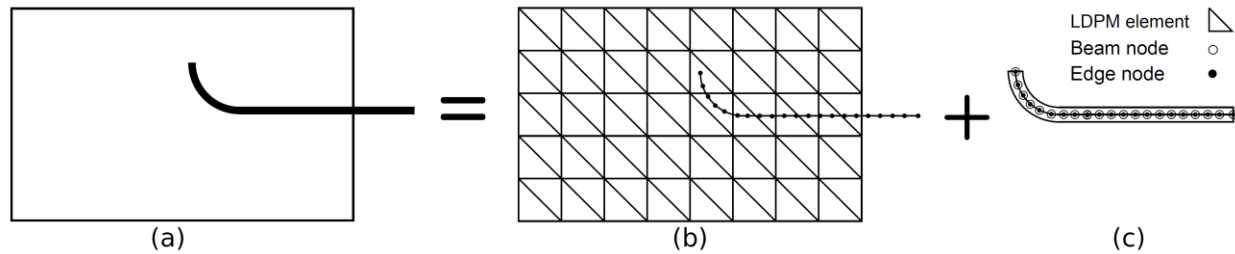


Figure 5. Kinematic model of fiber pullout test. (a) concrete specimen and fiber; (b) master-slave constraint between matrix (LDPM mesh) and fiber tunnel (geometric edge list); (c) penalty constraint between tunnel edge list and fiber (beam list).

In the current bond-slip constitutive model, the formulation is described by slippages in axial (S_a), radial (S_r), and circumferential (S_c) directions, and the corresponding stresses ($\sigma_a, \sigma_r, \sigma_c$) are calculated based on either elastic behavior or inelastic behavior as follows. For elastic behavior, the stresses are calculated as follows $\sigma_a = S_a K_a$, $\sigma_r = S_r K_r$, $\sigma_c = S_c K_c$, where $K_a = \alpha b_{10} / S_{10}$ is the axial stiffness, $K_r = p K_a$ is the radial stiffness, $K_c = p K_a$ is the circumferential stiffness, α is the bond shape parameter, b_{10} is the bond strength, S_{10} is slippage for elastic limit, and p is the penalty coefficient. b_{10} is the initial value of b_1 ; the same convention applies to b_{30} , S_{10} , S_{20} and S_{30} . Under inelastic behavior, the circumferential stress is computed

the same way as the elastic case. To describe the radial stress, an expansion parameter μ_N is introduced as the following:

$$\mu_N = \begin{cases} \mu_{N0} & S_a^* < S_{20} \\ \mu_{N0}(S_{30} - S_a^*) / (S_{30} - S_{20}) & S_{20} \leq S_a^* < S_{30} \\ 0 & S_a^* \geq S_{30} \end{cases} \quad (1)$$

where μ_{N0} is the initial expansion parameter, S_a^* is the absolute axial slippage, S_{20} is the slippage threshold at which bond begins to fail and starts to transition to frictional behavior, S_{30} is the max allowed slippage value at which bond is lost and only frictional behavior is remaining. Then radial stress can be written as $\sigma_r = K_r(S_r - \mu_N S_a^*)$. More details about the formulation can be found in Zhou et al. 2016.

Three types of experiments conducted at University of Maine to study the effects of embedment length, adjacent fibers and pulling angle were used for calibration and validation (Flanders, 2014). In our numerical analysis, concrete blocks of 10 mm × 10 mm × 16 mm are used. To validate the fiber-matrix interaction model proposed by this work, we simulated the single hooked fiber pullout, with embedment length of 6.35 mm, 9 mm and 12.7 mm, as shown in Figure 6. With the calibrated bond law parameters, the simulation results match the experiment results well, even in the post-peak. As the embedment length increases from 6.35 mm to 12.7 mm, the pullout peak load increases from about 150 N to about 250 N.

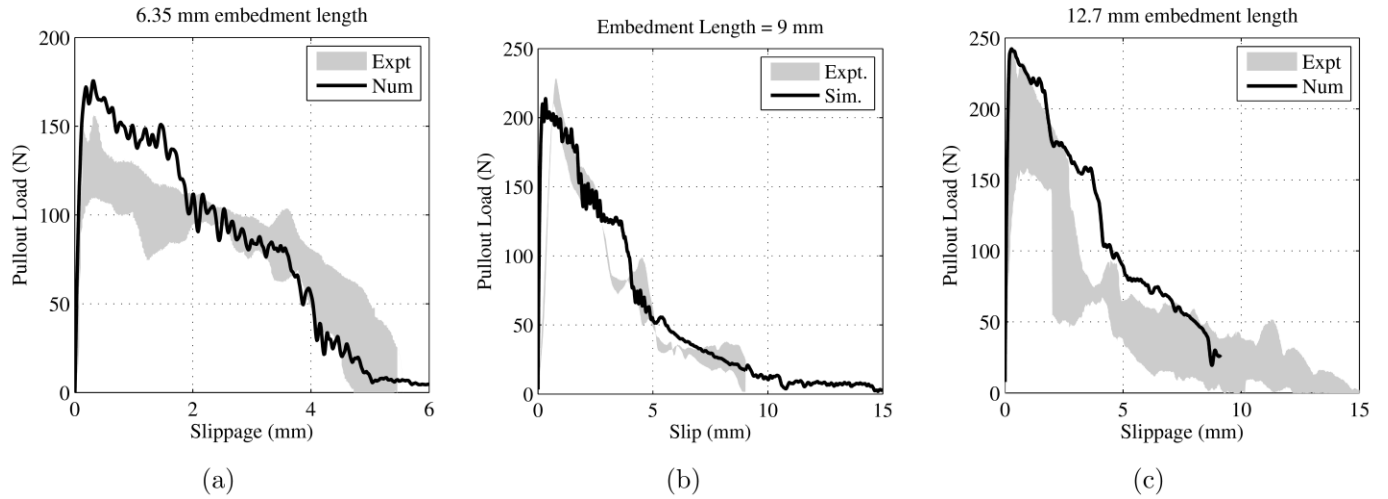


Figure 6. Effects of embedment length: (a) 6.35 mm embedment length, (b) 9 mm embedment length, and (c) 12.7 mm embedment length.

Conclusions

Tensile fiber pullout tests have been designed and conducted on CORTUF in this study. The results for three different configurations are presented and discussed. The high fidelity analytical model presented in this paper is shown to successfully capture various mechanisms in fiber-matrix interaction. Numerical studies reveal that the current model is also capable of simulating the mechanical deformation of hooked fibers during pullout and accurately predicting the effects of different embedment lengths.

References

- Alwan, J.M., Naaman, A.E., and Guerrero, P. “Effect of mechanical clamping on the pullout response of hooked steel fibers embedded in cementitious matrices.” *Concr. Sci. Eng.* Vol. 1, No. 1, March 1999, pp. 15-25.
- Banthia, N., and Trottier, J.F. “Concrete reinforced with deformed steel fibers, Part I: Bond-slip mechanisms.” *ACI Materials Journal* Vol. 91, No. 5, September 1994, pp. 435-446.
- Cantwell, W.J., and Morton, J. “The impact resistance of composite materials-review.” *Composites* Vol. 22, No. 5, September 1991, pp. 347-362.
- Cusatis, G., Schaufert, E.A., Pelessone, D., O’Daniel, J.L., Marangi, P., Stacchini, M., Savoia, M. “Lattice discrete particle model for fiber reinforced concrete (LDPM-F) with application to the numerical simulation of armoring systems.” Proc., Computational Modelling of Concrete Structures (EURO-C 2010), Taylor and Francis, London.
- Cusatis, G., Pelessone, D., Mencarelli, A. “Lattice discrete particle model (LDPM) for failure behavior of concrete. I: Theory.” *Cem. Concr. Compos.* Vol. 33, No. 9, October 2011a, pp. 881-890.
- Cusatis, G., Pelessone, D., Mencarelli, A., Baylot, J. “Lattice discrete particle model (LDPM) for failure behavior of concrete. II: Calibration and validation.” *Cem. Concr. Compos.* Vol. 33, No. 9, October 2011b, pp. 891-905.
- Ezeldin, S., and Lowe, S.R. “Mechanical properties of steel fibre reinforced rapid-set materials.” *ACI Mater J* Vol. 88, No. 4, July 1991, pp. 384-9.
- Flanders, L.S. “A 3d image analysis of energy dissipation mechanisms in ultra high performance fiber reinforced concrete subject to high loading rates,” Master’s thesis, Department of Civil & Environmental Engineering, University of Maine, December 2014.
- Georgiadi-Stefanidi, K., Mistakidis, E., Pantousa, D., Zygomas, M. “Numerical modelling of the pull-out of hooked steel fibres from high-strength cementitious matrix, supplemented by experimental results.” *Construction and Building Materials*, Vol. 24, No. 12, December 2010, pp. 2489-2506.
- Hughes, B.P. and Fattuhi, N.I. “Fiber bond strengths in cement and concrete.” *Magazine of Concrete Research* Vol. 27, No. 92, September 1975, pp. 161-166.
- Laranjeira, F., Aguado, A., and Molins, C. “Predicting the pullout response of inclined straight steel fibers.” *Materials and Structures* Vol. 43, No. 6, July 2010, pp. 875-895.
- Lee, Y., Kang, S.T., and Kim, J.K. “Pullout behavior of inclined steel fiber in an ultra-high strength cementitious matrix.” *Construction and Building Materials* Vol. 24, No. 10, October 2010, pp. 2030-2041.

Leung, C.K.Y., and Shapiro, N. “Optimal steel fiber strength for reinforcement of cementitious materials.” *Journal of Materials in Civil Engineering* Vol. 11, No. 2, May 1999, pp. 116-123.

Naaman, A.E., Namur, G.G., Alwan, J.M., and Najm, H.S. “Fiber pullout and bond slip. I: Analytical study.” *Journal of Structural Engineering* Vol. 117, No. 9, September 1991, pp. 2769-2790.

Roth, M.J., Rushing, T.S., Flores, O.G., Sham, D.K., Stevens, J.W. “Laboratory investigation of the characterization of cortuf flexural and splitting tensile properties.” Technical Report. Vicksburg, MS: US Army Corps of Engineers, Engineer Research and Development Center; September 2009, pp. 1-57.

Schauffert, E.A., Cusatis, G. “Lattice discrete particle model for fiber-reinforced concrete. I: Theory.” *J. Eng. Mech.* Vol. 138, No. 7, July 2012a, pp. 826-833.

Schauffert, E.A., Cusatis, G., Pelessone, D., O’Daniel, J., Baylot, J. “Lattice Discrete Particle Model for fiber reinforced concrete (LDPM-F): II Tensile fracturing and multiaxial loading behavior.” *J. Eng. Mech.* Vol. 138, No. 7, July 2012b, pp. 834-841.

Sujivorakul, C., Waas, A.M., Naaman, A.E. “Pullout response of a smooth fiber with an end anchorage.” *J. Eng. Mech.* Vol. 126, No. 9, September 2000, pp. 986-993.

Zhou, X., Feng, J., Flanders, L., Landis, E., Pelessone, D., Baylot, J., Cusatis, G. “Micro-mechanical characterization of hooked fiber-matrix interaction for ultra-high performance concrete: numerical modeling and experimental validation.” To be submitted, 2016.